Int. J. Electrochem. Sci., 7 **(2012)** 1187 - 1195

International Journal of
ELECTROCHEMICAL
SCIENCE
www.electrochemsci.org

Electrophoretic Deposition of Poly(*N*-Vinyl-2-Pyrrolidone)-Capped Platinum Nanoparticles on Fluorine-Doped Tin Oxide Glass as a Counter Electrode for Dye-Sensitized Solar Cells

Mao-Sung Wu[*] *and Yu-Jun Zheng*

Department of Chemical and Materials Engineering, National Kaohsiung University of Applied Sciences, Kaohsiung 807, Taiwan
[*]E-mail: ms_wu@url.com.tw

Received: 1 December 2011 / *Accepted:* 12 January 2012 / *Published:* 1 February 2012

Pt nanoparticles (about 1.8 nm in diameter) protected with a polymer layer are prepared by a chemical reduction of Pt ions in the presence of PVP [poly(*N*-vinyl-2-pyrrolidone)]. PVP-capped Pt nanoparticles can be well dispersed in an isopropyl alcohol solution due to the electrostatic repulsion between Pt nanoparticles and steric repulsion between the adsorbed PVP layers. An ultrathin layer of PVP-capped Pt nanoparticles is homogeneously deposited onto the fluorine-doped tin oxide (FTO) glass by electrophoretic deposition (EPD). The photoelectron conversion efficiency of the dye-sensitized solar cell is increased from 0.02 to 6.00% after employing the cathode with ultrathin transparent Pt layer prepared by EPD.

Keywords: Polymer-capped nanoparticles, dye-sensitized solar cell, electrophoretic deposition, Pt nanoparticles, and transparent film

1. INTRODUCTION

Dye-sensitized solar cell (DSC), which is a device converting light to electricity, has attracted much research attention due to its simplicity and low fabrication cost [1]. The photoanode of DSC is typically made of a dye-sensitized mesoporous TiO_2 layer which is coated on the fluorine-doped tin oxide (FTO) glass [2,3]. The electrolyte contains a redox couple (I^-/I_3^-) in organic solvents or ionic liquid [4]. Platinum is a widely used cathode material due to its high electrocatalytic activity towards the reduction of triiodide. The platinized cathode may play an important role in enhancing the photovoltaic properties of DSCs. The cathode material is required to provide high electrocatalytic activity, indicating that the available catalytic surface in cathode plays a crucial role in determining

cell performance. It is generally believed that the nanostructured platinum such as nanoparticle favors the photoelectron conversion efficiency of DSCs because it can provide large surface area for triiodide reduction [5].

The Pt nanoparticle preparation and its deposition onto the FTO surface determine the final film structure/property and ultimately the final cell performance. Various synthetic methods such as thermal decomposition [6,7], polyol method [7-9], and chemical reduction [10,11] have been employed to prepare the Pt nanoparticles for DSCs. Among these methods, thermal decomposition has been a common synthetic method to obtain a reliable thin Pt coating layer for improving the cell performance [6].

In addition to the synthesis of Pt nanoparticles, the formation of Pt thin layer on the FTO surface is also an important process affecting the cell performance. Several processes including sputtering [12,13], dip coating [14,15], screen printing [7], electrophoretic deposition [16], electroless deposition [17,18], and electrodeposition [19-23] have been used to fabricate Pt layer on the FTO surface. Previous reports indicated that the Pt nanoparticles protected with a polymer such as PVP [poly(*N*-vinyl-2-pyrrolidone)] show superior dispersion stability in the aqueous solutions [14,24]. In this work, we propose an electrophoretic deposition (EPD) strategy allowing fast fabrication of PVP-capped Pt nanoparticles on the FTO surface.

The amount of Pt loading can be controlled by tuning the deposition parameters such as voltage, current density, temperature, and bath composition. The photovoltaic properties of DSCs employing Pt-coated cathode were characterized.

2. EXPERIMENTAL

PVP-capped Pt nanoparticles were synthesized by the dissolving 0.1 g PVP (average molecular weight = 8000 g mol^{-1}) in an isopropyl alcohol (IPA) solution (44 mL) at room temperature. H_2PtCl_6 (0.0205 g) as a precursor was added to the prepared PVP solution. 0.5 M $NaBH_4$ solution (1 mL) as a reductant was then added slowly and stirred with the mixture in a beaker. The solution instantaneously changed from yellowish to black, indicating the formation of Pt nanoparticles. EPD of PVP-capped Pt nanoparticles was carried out in the PVP-capped Pt suspension by applying a voltage difference of 30 V between FTO glass (3.1 mm thick, 13 Ω/□, Nippon Sheet Glass) and platinum (2 cm × 2 cm) electrodes for various periods of time to obtain the required weight. Prior to deposition, FTO glass was cut into pieces of 1.5 cm × 1.5 cm, soaked in acetone and ultrasonic vibrated for 20 min to wash away any contaminants off the surface.

Deionized water was then used to rinse the FTO in ultrasonic vibration for another 15 min. For comparison, the Pt-coated FTO electrode was also obtained by dip-coating PVP-capped Pt nanoparticles directly onto the FTO followed by drying at 100ºC for 3 min. The dip-coating process was repeated several times to obtain the required weight. After deposition, the PVP-capped FTO electrodes were heat-treated at 425°C for 15 min to remove the PVP. The surface morphology of the Pt-coated FTO electrodes was examined with a field-emission electron microscope (FE-SEM, Jeol JEOL-6330). The nanostructure of the Pt nanoparticles was characterized by a transmission electron

microscopy (FE-TEM, JEOL JEM-1400) with an accelerating voltage of 200 kV. The optical transmittance of the Pt-coated FTO electrodes was measured with an ultraviolet-visible spectrometer (UV-Vis, PerkinElmer Lambda 35).

TiO_2 photoanodes were prepared by screen printing the TiO_2 paste on the FTO-coated glass substrate [25,26]. The thickness of the resultant TiO_2 films was approximately 15 μm measured by the profiler.

The adsorption of dye on the TiO_2 surface was carried out by soaking the TiO_2 photoanodes in a dry ethanol solution of N719 dye for 12 h at room temperature. A dye-coated photoanode was assembled with a Pt-coated FTO glass cathode by using a sealing plastic to form a sandwich-type DSC. An electrolyte containing 0.6 M 1-propyl-2,3-dimethylimidazolium iodide, 0.1 M lithium iodide, 0.05 M iodine, and 0.5 M 4-tert-butylpyridine in MPN (3-methoxypropionitrile) solvent was then infiltrated into voids between the two electrodes of the DSC.

The active area of DSCs was 0.283 cm^2. The photocurrent-voltage characteristics under one-sun illumination (AM1.5, 100 mW cm^{-2}) were carried out by scanning DSCs from the open-circuit voltage of the cell to the short-circuit condition at a scan rate of 5 mV s^{-1} with a source meter (Keithley 2400). All chemicals used were of analytical grade and were used as received without further purification.

3. RESULTS AND DISCUSSION

Figure 1 illustrates the formation of PVP-capped Pt nanoparticles on FTO surface using electrophoretic deposition. PVP-capped Pt nanoparticles can be well dispersed in an IPA solution due to the electrostatic repulsion between positively charged Pt nanoparticles and steric repulsion between the adsorbed PVP layers. EPD of PVP-capped Pt layer is achieved via transport of positively charged Pt nanoparticles toward a negative electrode (FTO) and deposition of nanoparticles under the applied electric field. When a PVP-capped Pt nanoparticle arrives at the FTO surface, the positive charges on the Pt nanoparticle can be electrochemically reduced, forming the PVP-capped Pt nanoparticle on the FTO surface.

PVP-capped Pt nanoparticles prefer to deposit at the exposed FTO/electrolyte interface rather than deposit at the PVP-capped Pt/electrolyte surface due to the steric repulsion between the adsorbed PVP layers. Therefore, a uniform layer with well dispersed Pt nanoparticles can be achieved by the electrophoresis of PVP-capped Pt nanoparticles.

Figure 2a shows the TEM micrograph of PVP-capped Pt nanoparticles. Clearly, the synthesized Pt nanoparticles have a very small particle size (1.83±0.44 nm). It is believed that Pt nanoparticles with small particle size can provide high catalytic surface for the triiodide reduction. However, the deposition process may affect the kinetic behavior of the Pt cathode due to the aggregation of Pt nanoparticles.

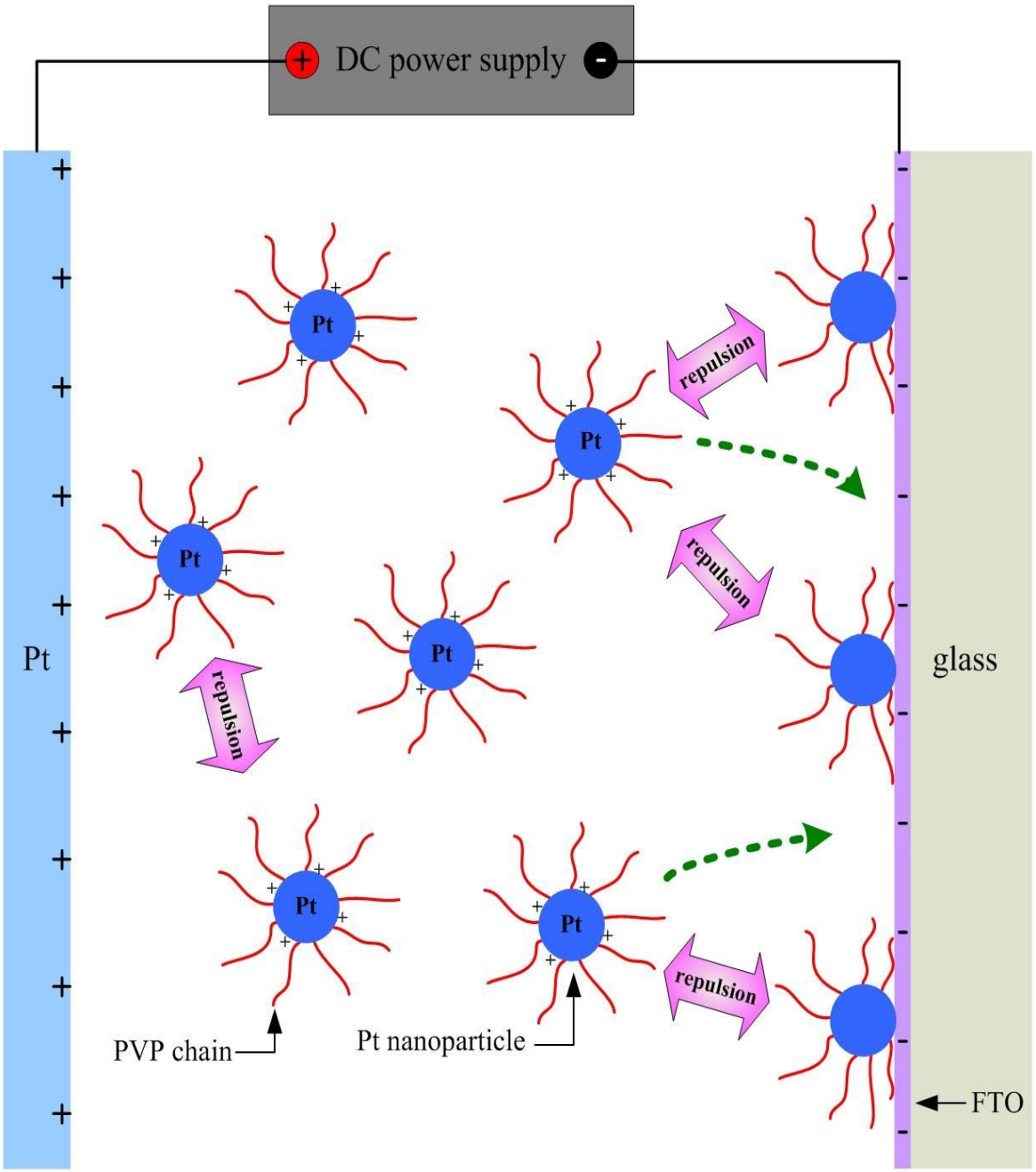

Figure 1. Schematic diagram illustrating the formation of PVP-capped Pt nanoparticles on FTO using electrophoretic deposition.

Figure 2b shows the surface morphology of bare FTO glass. By use of dip-coating process, a large amount of aggregated Pt nanoparticles approximately 5-10 nm in diameter can be observed on the FTO after 12 dipping cycles shown in Figure 2c. Previous report indicated that the aggregated Pt nanoparticles can be obtained by using a two-step dip-coating process [14]. Figure 2d shows the SEM micrograph of Pt nanoparticles coated on the FTO by EPD for 240 s. Interestingly, it is difficult to detect the aggregated Pt nanoparticles using SEM, meaning that an ultrathin layer of well dispersed Pt nanoparticles can be achieved by the electrophoretic deposition strategy.

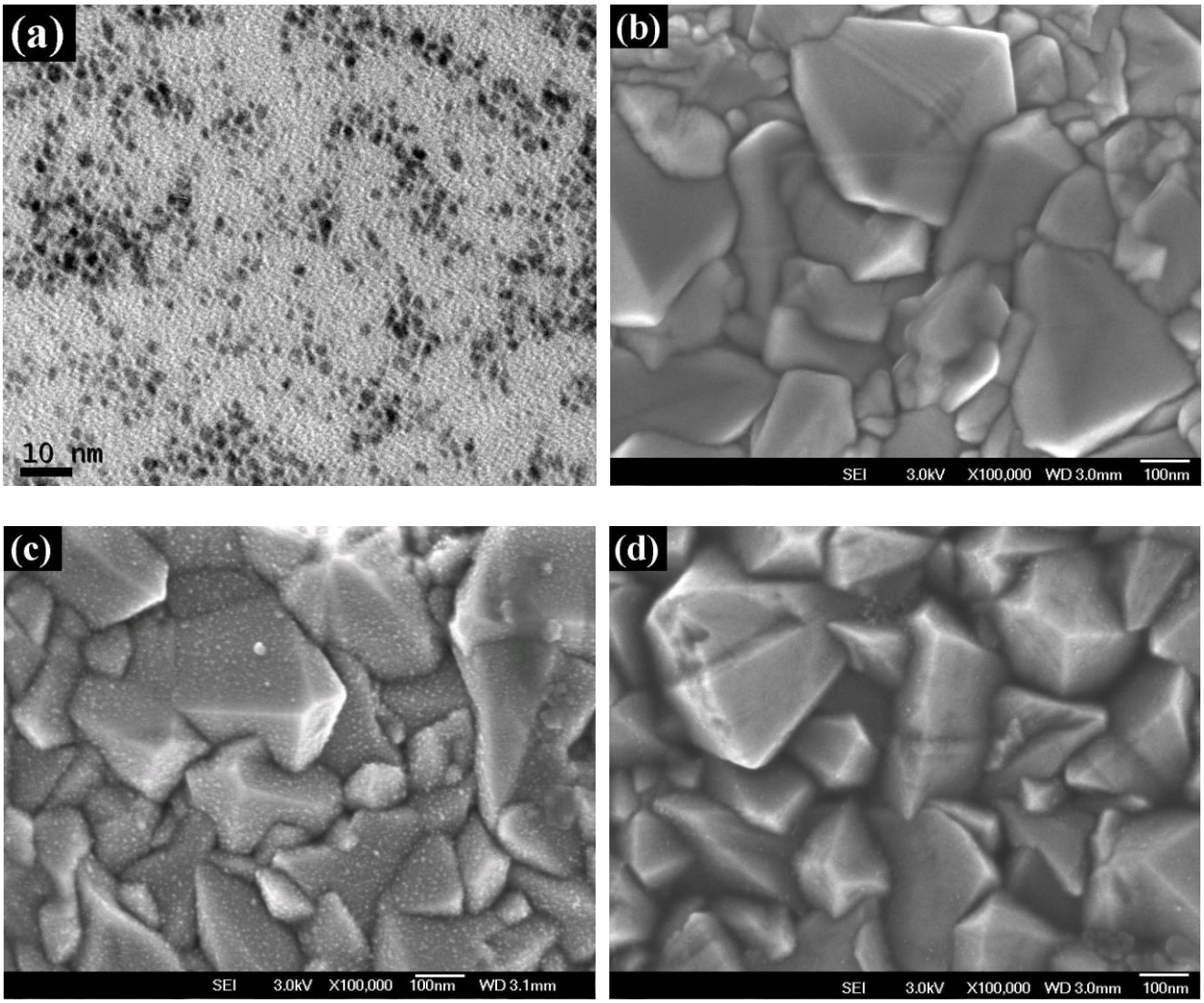

Figure 2. (a) TEM micrograph of PVP-capped Pt nanoparticles before annealing. SEM micrograph of (b) bare FTO, (c) Pt-coated FTO obtained by dip-coating method, and (d) Pt-coated FTO obtained by EPD. All samples were annealed at 425ºC for 15 min before SEM observations.

Figure 3 shows the photocurrent-voltage (*J-V*) characteristics of the DSCs employing the Pt-coated FTO cathodes prepared by dip-coating and EPD methods. The dip-coating process was repeated 12 times. EPD was performed for 240 s. The photovoltaic properties of DSC using Pt-coated FTO prepared by EPD method were superior to those of DSC using Pt-coated FTO prepared by dip-coating method. The resulting photovoltaic parameters derived from *J-V* curves are tabulated in Table 1. When a bare FTO glass was used as the cathode, the open-circuit voltage (V_{oc}) of the DSC was only 0.48 V, the short-circuit current density (J_{sc}) was about 0.55 mA cm^{-2}, the fill factor (*FF*) was 5.8%, and the photoelectron conversion efficiency (η) was only 0.02%. Such low conversion efficiency resulted from the lack of catalytic activity of the bare FTO for triiodide reduction. When the Pt nanoparticles were coated onto FTO by EPD for 10 s, the V_{oc}, J_{sc}, and *FF* were significantly increased to 0.69 V, 13.36 mA cm^{-2}, and 53.3%, respectively. The conversion efficiency achieved was up to 4.87%. This result means that the charge-transfer resistance at the electrolyte/cathode interface is significantly decreased,

due to the catalytic activity of the Pt layer on the FTO glass. It turned out that the catalytic activity of the Pt layer is a crucial factor in enhancing the performance of DSCs. η of the DSC increases with increasing the number of dipping cycle or EPD time and eventually level off.

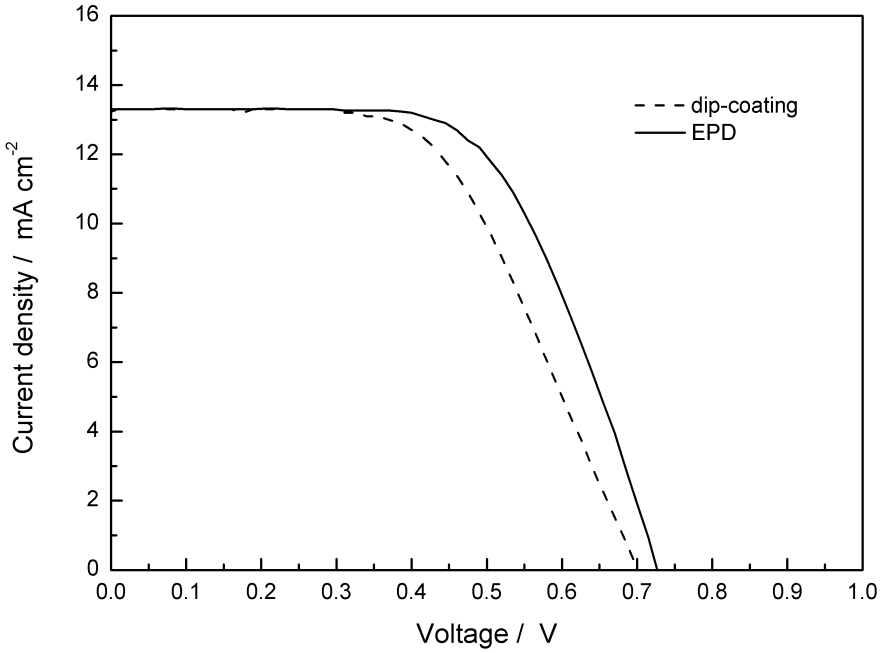

Figure 3. Photocurrent-voltage (*J-V*) characteristics of the DSSCs employing the Pt-coated FTO cathodes prepared by dip-coating and EPD methods. All cathodes were annealed at 425ºC for 15 min before measurements.

Table 1. Photovoltaic parameters obtained from the photocurrent-voltage curves of DSCs using Pt cathodes prepared by EPD and dip-coating methods.

EPD time (s)	**J_{sc} (mA cm^{-2})**	**V_{oc} (V)**	**fill factor (%)**	**η (%)**
0	0.55	0.48	5.8	0.02
10	13.36	0.69	53.3	4.87
30	12.93	0.73	57.0	5.38
60	12.95	0.71	59.9	5.51
120	13.50	0.72	59.1	5.75
240	13.51	0.73	60.8	6.00
300	13.02	0.73	62.0	5.89
No. of dipping cycle	J_{sc} (mA cm^{-2})	V_{oc} (V)	fill factor (%)	η (%)
0	0.55	0.48	5.8	0.02
1	13.60	0.68	39.5	3.65
3	13.49	0.70	46.8	4.42
6	13.54	0.70	50.4	4.78
12	13.23	0.70	53.0	4.91

The catalytic activity of the Pt layer may be reduced and saturated due to the agglomeration of the Pt nanoparticles under the long EPD times or numerous dipping cycles. Therefore, it is clear that no improvement of performance is achieved for the DSC coated with a thick Pt layer on FTO. In addition, the optimal η of DSC employing EPD-coated Pt cathode (6.0%) was higher than that of DSC employing dip-coated Pt cathode (4.9%), probably due to the well dispersed Pt nanoparticles on the FTO prepared by EPD method. The photoelectron conversion efficiency of DSC employing EPD-coated Pt cathode is higher than that of DSC with Pt cathode prepared by a two-step dip coating [14,15] and lower than that of DSC with Pt cathode deposited by a chemical deposition method [17].

Figure 4 shows the UV-Vis absorption spectra of bare FTO and Pt-coated FTO electrodes prepared by EPD for various deposition times. There is no apparent difference in transmittance between the bare FTO and Pt-coated FTO. The mean light transmittances of bare FTO and Pt-coated FTO electrodes were measured between 500 nm and 800 nm. It is surprising to find that the Pt-coated FTO by EPD for 10 s has a mean transmittance as high as 78.8% in the visible light region, which is only slightly lower than that of the bare FTO substrate (79.7%). The ultrathin and well dispersed Pt layer prepared by EPD was responsible for the high transmittance. When increasing the deposition time to 240 s, the transmittance of Pt-coated electrode slightly decreases to 77.0%. Therefore, EPD features easy and fast fabrication of ultrathin transparent layer with well dispersed Pt nanoparticles from a suspension of PVP-capped Pt nanoparticles.

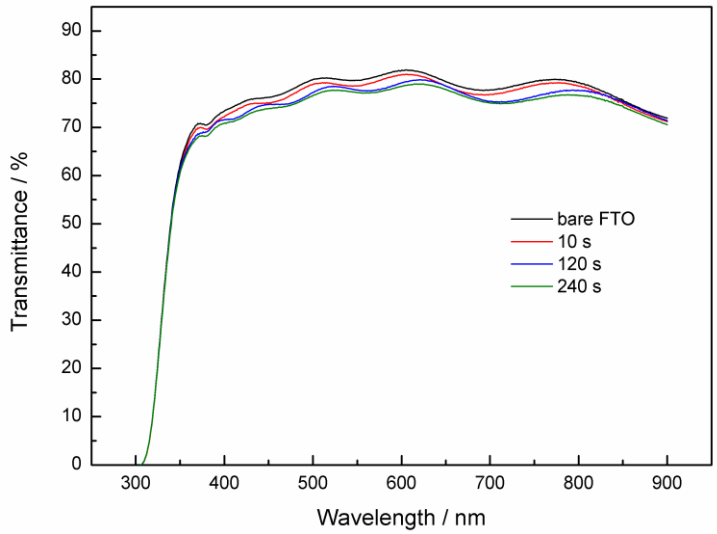

Figure 4. UV-Vis absorption spectra of the bare FTO and Pt-coated FTO glass electrodes prepared by EPD for various deposition times. The Pt-coated FTO electrodes were annealed at 425ºC for 15 min before measurements.

4. CONCLUSIONS

EPD of PVP-capped Pt nanoparticles occurs at the exposed FTO/electrolyte interface due to the steric repulsion between the adsorbed PVP layers. In addition, it is difficult to conduct electrons from

the FTO to the outer layer of the PVP-capped Pt nanoparticles. Therefore, a single layer of well dispersed Pt nanoparticles is likely to be deposited on the FTO by the electrophoresis of PVP-capped Pt nanoparticles. The transmittance of ultrathin Pt layer prepared by EPD is slightly lower than that of bare FTO glass in the visible light region. A DSC employing the ultrathin transparent Pt-coated FTO showed a high energy-conversion efficiency of about 6%. The enhanced photovoltaic properties could be attributed to the well dispersed Pt nanoparticles which provide high catalytic activity for triiodide reduction. The proposed EPD strategy is important for reducing production cost by reducing the fabrication time and required amount of expensive Pt.

ACKNOWLEDGEMENTS
The authors gratefully acknowledge the financial support from the National Science Council, Taiwan, Republic of China (Project No: NSC 100-2221-E-151-059).

References

1. B. O'Regan and M. Gratzel, *Nature*, 353 (1991) 737-740.
2. T.-H. Tsai, S.-C. Chiou and S.-M. Chen, *Int. J. Electrochem. Sci*., 2011 (2011) 3333-3343.
3. V. Baglio, M. Girolamo, V. Antonucci and A.S. Aricò, *Int. J. Electrochem. Sci*., 6 (2011) 3375-3384.
4. S.-Y. Ku and S.-Y. Lu, *Int. J. Electrochem. Sci*., 6 (2011) 5219-5227.
5. P. Calandra, G. Calogero, A. Sinopoli and P.G. Gucciardi, *Int. J. Photoenergy*, 2010 (2010) 1-15.
6. N. Papageorgiou, W.F. Maier and M. Gratzel, *J. Electrochem. Soc*., 144 (1997) 876-884.
7. G. Khelashvili, S. Behrens, C. Weidenthaler, C. Vetter, A. Hinsch, R. Kern, K. Skupien, E. Dinjus and H. Bonnemann, *Thin Solid Films*, 511-512 (2006) 342-348.
8. K. Sun, B. Fan and J. Ouyang, *J. Phys. Chem. C*, 114 (2010) 4237-4244.
9. S.J. Cho and J. Ouyang, *J. Phys. Chem. C*, 115 (2011) 8519-8526.
10. P. Li, J. Wu, J. Lin, M. Huang, Y. Huang and Q. Li, *Sol. Energy*, 83 (2009) 845-849.
11. G. Calogero, P. Calandra, A. Irrera, A. Sinopoli, I. Citro and G. Di Marco, *Energy Environ. Sci*., 4 (2011) 1838-1844.
12. X. Fang, T. Ma, G. Guan, M. Akiyama, T. Kida and E. Abe, *J. Electroanal. Chem*., 570 (2004) 257-263.
13. Y.-L. Lee, C.-L. Chen, L.-W. Chong, C.-H. Chen, Y.-F. Liu and C.-F. Chi, *Electrochem. Commun*., 12 (2010) 1662-1665.
14. T.C. Wei, C.C. Wan and Y.Y. Wang, *Appl. Phys. Lett*., 88 (2006) 103122.
15. J.-L. Lan, Y.-Y. Wang, C.-C. Wan, T.-C. Wei, H.-P. Feng, C. Peng, H.-P. Cheng, Y.-H. Chang and W.-C. Hsu, *Curr. Appl. Phys*., 10 (2010) S168-S171.
16. X. Yin, Z. Xue and B. Liu, *J. Power Sources*, 196 (2011) 2422-2426.
17. C.-M. Chen, C.-H. Chen and T.-C. Wei, *Electrochim. Acta*, 55 (2010) 1687-1695.
18. C.-Y. Lin, J.-Y. Lin, J.-L. Lan, T.-C. Wei and C.-C. Wan, *Electrochem. Solid-State Lett*., 13 (2010) D77-D79.
19. S. Kim, Y. Nah, Y. Noh, J. Jo and D. Kim, *Electrochim. Acta*, 51 (2006) 3814-3819.
20. P. Li, J. Wu, J. Lin, M. Huang, Z. Lan and Q. Li, *Electrochim. Acta*, 53 (2008) 4161-4166.
21. G. Tsekouras, A.J. Mozer and G.G. Wallace, *J. Electrochem. Soc*., 155 (2008) K124-K128.
22. C. Yoon, Rvittal, J. Lee, W. Chae and K. Kim, *Electrochim. Acta*, 53 (2008) 2890-2896.

23. C.-Y. Lin, J.-Y. Lin, C.-C. Wan and T.-C. Wei, *Electrochim. Acta*, 56 (2011) 1941-1946.
24. J.-L. Lan, C.-C. Wan, T.-C. Wei, W.-C. Hsu, C. Peng, Y.-H. Chang and C.-M. Chen, *Int. J. Electrochem. Sci*., 6 (2011) 1230-1236.
25. M.S. Wu, C.H. Tsai and T.C. Wei, *Chem. Commun*., 47 (2011) 2871-2873.
26. M.-S. Wu, C.-H. Tsai, J.-J. Jow and T.-C. Wei, *Electrochim. Acta*, 56 (2011) 8906-8911.